Byrnes and Slep, https://doi.org/10.1083/jcb.201610090

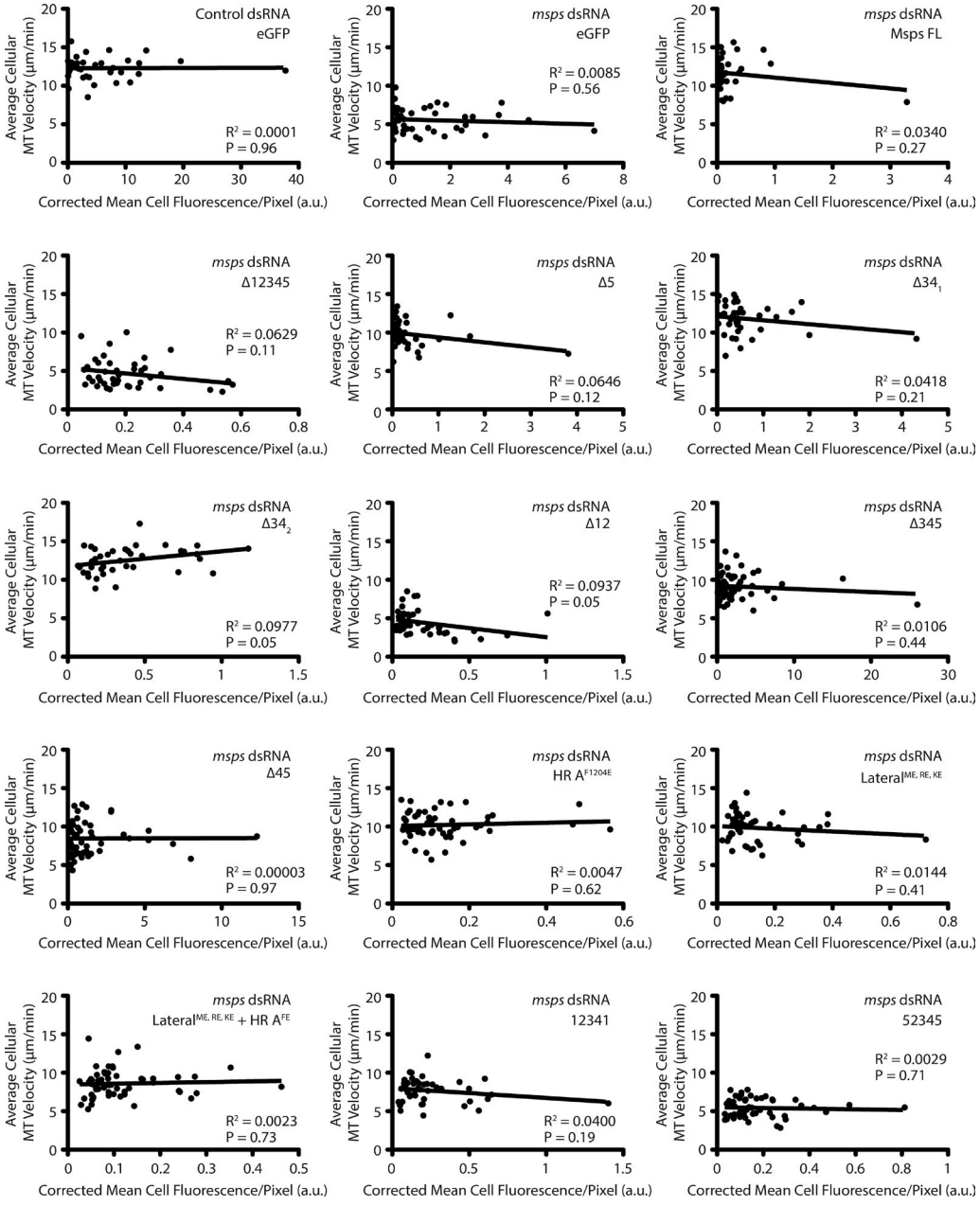

Figure S1. **Msps-eGFP construct expression does not correlate with EB1-tRFP comet velocity.** Corrected mean cell fluorescence/pixel was calculated for cells expressing eGFP and the 13 Msps-eGFP constructs used in EB1-tRFP MT polymerization rescue experiments. Msps-eGFP or eGFP (control) expression levels do not correlate with the corresponding EB1 comet velocities measured.

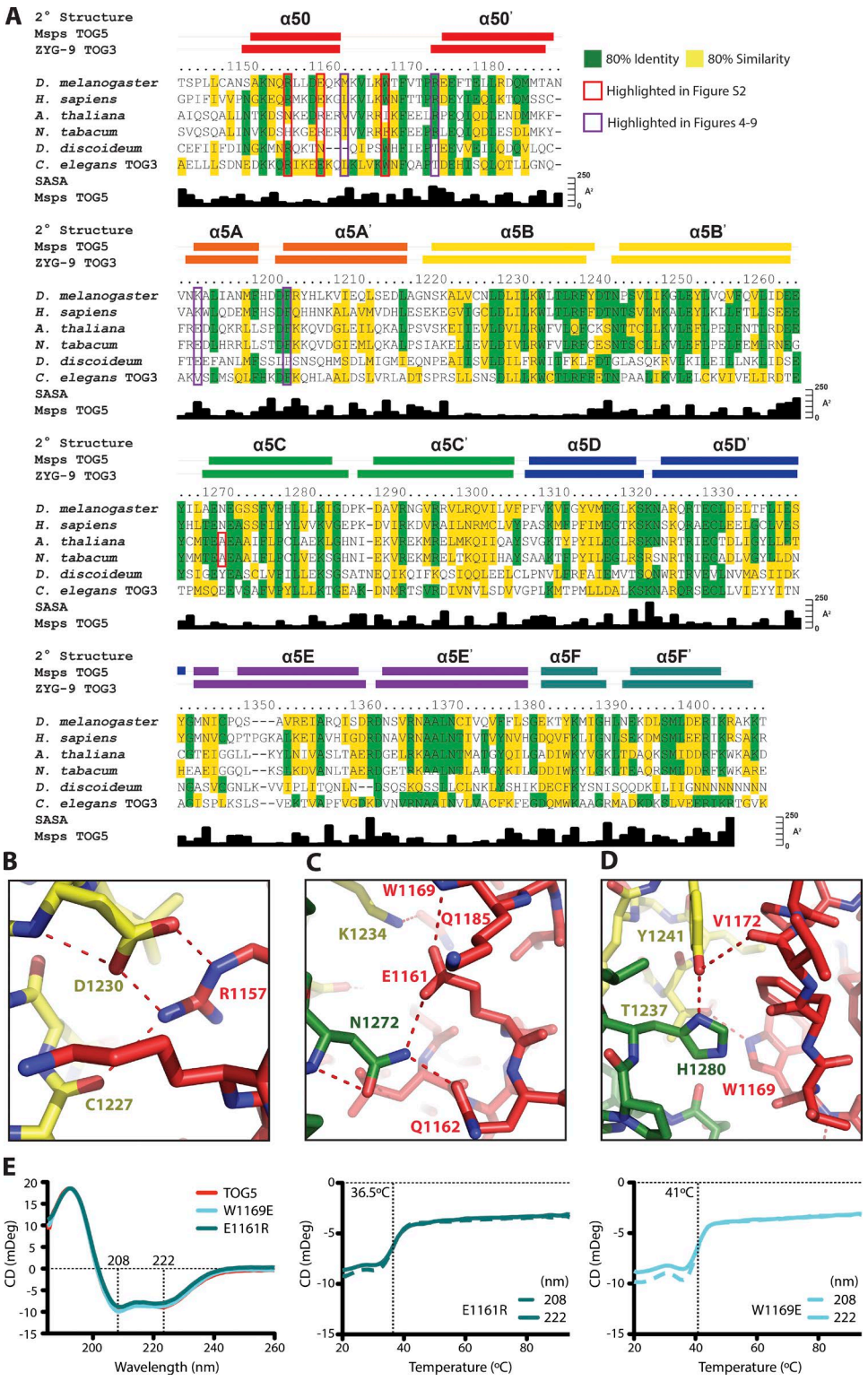

Figure S2. **TOG5 is structurally conserved and contains a stabilizing N-terminal HR.** (A) Sequence alignment of TOG5 domains and ZYG-9 TOG3. Conservation is mapped based on a multispecies alignment, with residues containing 80% identity and similarity highlighted in green and yellow, respectively. Solvent-accessible surface area and residue numbers correspond to the Msps TOG5 structure. Residues boxed in red and purple correspond to domain stability analyses (B–E) and HR 0–A mechanistic analyses (Figs. 4–9), respectively. The secondary structures of Msps TOG5 and ZYG-9 TOG3 (2OF3) are presented above the alignment. (B–E) HR 0 makes contacts with HRs A–C that contribute to domain stability. Conserved residues including R1157 (B), E1161 (C), and W1169 (D) make contact with the body of TOG5. (E) CD spectra of native (red), E1161R (blue), and W1169E (cyan) TOG5 constructs display minima at 208 and 222 nm, consistent with α-helical secondary structure. CD thermal melting data indicate that mutating residues in HR 0 differentially affect TOG5 domain stability, although not dramatically. E1161R (middle) lowers the thermal melting of TOG5 from 42°C (Fig. S4 C) to 36.5°C, but a W1169E mutation (right) does not appreciably change TOG5 domain stability. We note that mutating R1157 completely destabilizes TOG5 and this construct cannot be purified from *E. coli*.

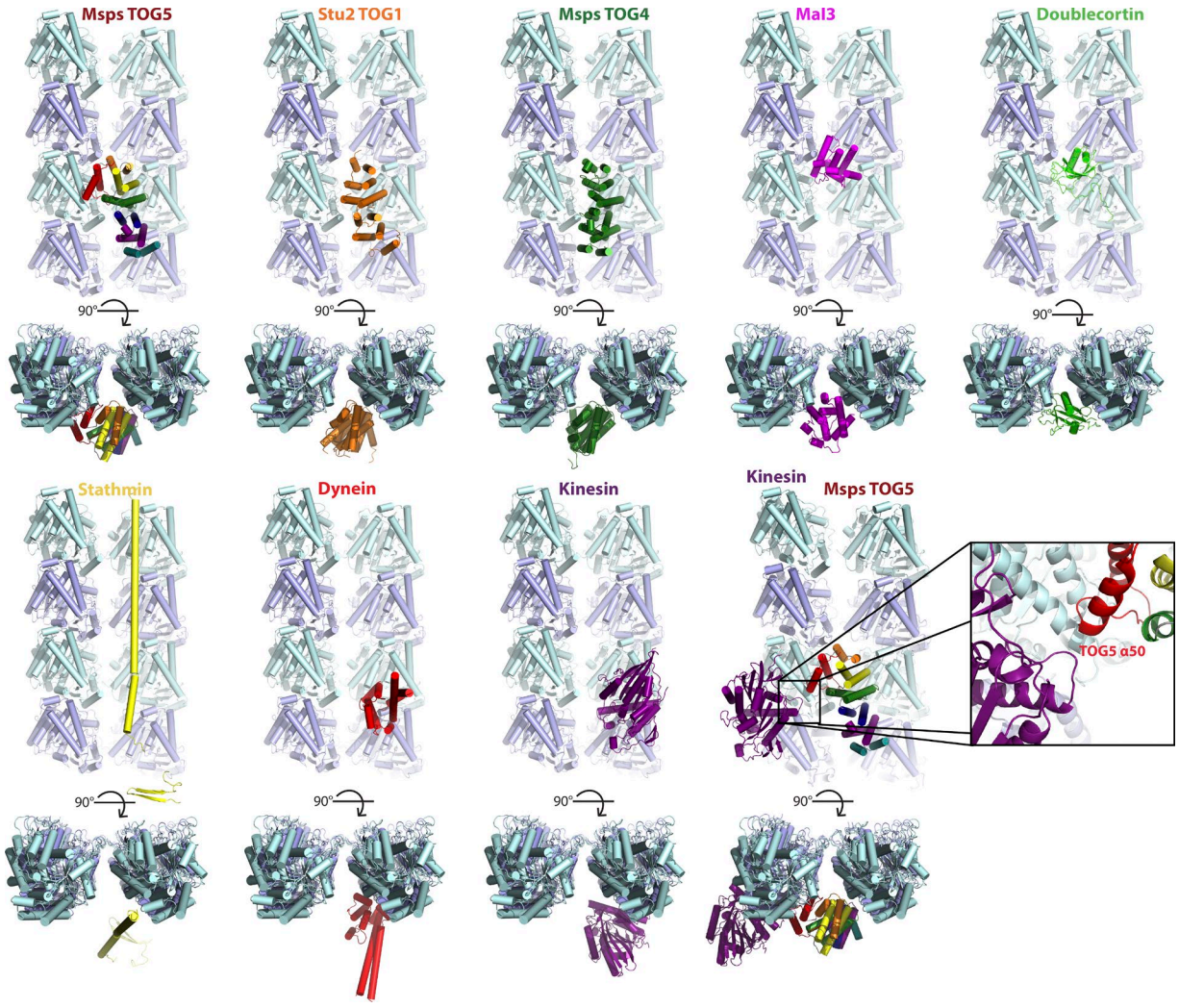

Figure S3. **MAPs contact the MT lattice in unique ways.** Using the Stu2 TOG1–tubulin (Ayaz et al., 2012; 4FFB) and Mal3-GTPγS–MT (Maurer et al., 2012; 4ABO) complex structures as guides, we modeled TOG domains on the MT lattice. TOGs 1–3 are not predicted to make lateral αβ-tubulin contacts; however, TOG4 (Fox et al., 2014; 4Y5J) is positioned to make contact with lateral α-tubulin. TOG5 HRs 0–A are positioned to engage β-tubulin and +1 α-tubulin on a neighboring protofilament. Other MAP–MT/tubulin complexes reveal distinct MAP–tubulin interactions that overlap, to varying degrees, with the predicted TOG–tubulin binding site. Mal3 (Maurer et al., 2012; 4ABO) and doublecortin (Liu et al., 2012; 4ATU) fenestrate between four heterodimers, positioning them to allosterically recognize tubulin's nucleotide state and lattice curvature. The interaction of TOG5 with lateral αβ-tubulin could inhibit Mal3 or doublecortin binding, as TOG5's predicted MT binding site overlaps with the MT binding sites of these MAPs. The potential lateral interaction of TOGs 4 and 5 differs from those of stathmin (Nawrotek et al., 2011; 3RYF), kinesin (Cao et al., 2014; 4LNU), and dynein (Redwine et al., 2012; 3J1T), which preferentially bind tubulin heterodimers along a single protofilament. We note that when kinesin is docked on a protofilament neighboring that which TOG5 is bound to, TOG5 HR 0 (red) nicely adjoins the neighboring kinesin motor domain and may potentially enable TOG5–kinesin interactions.

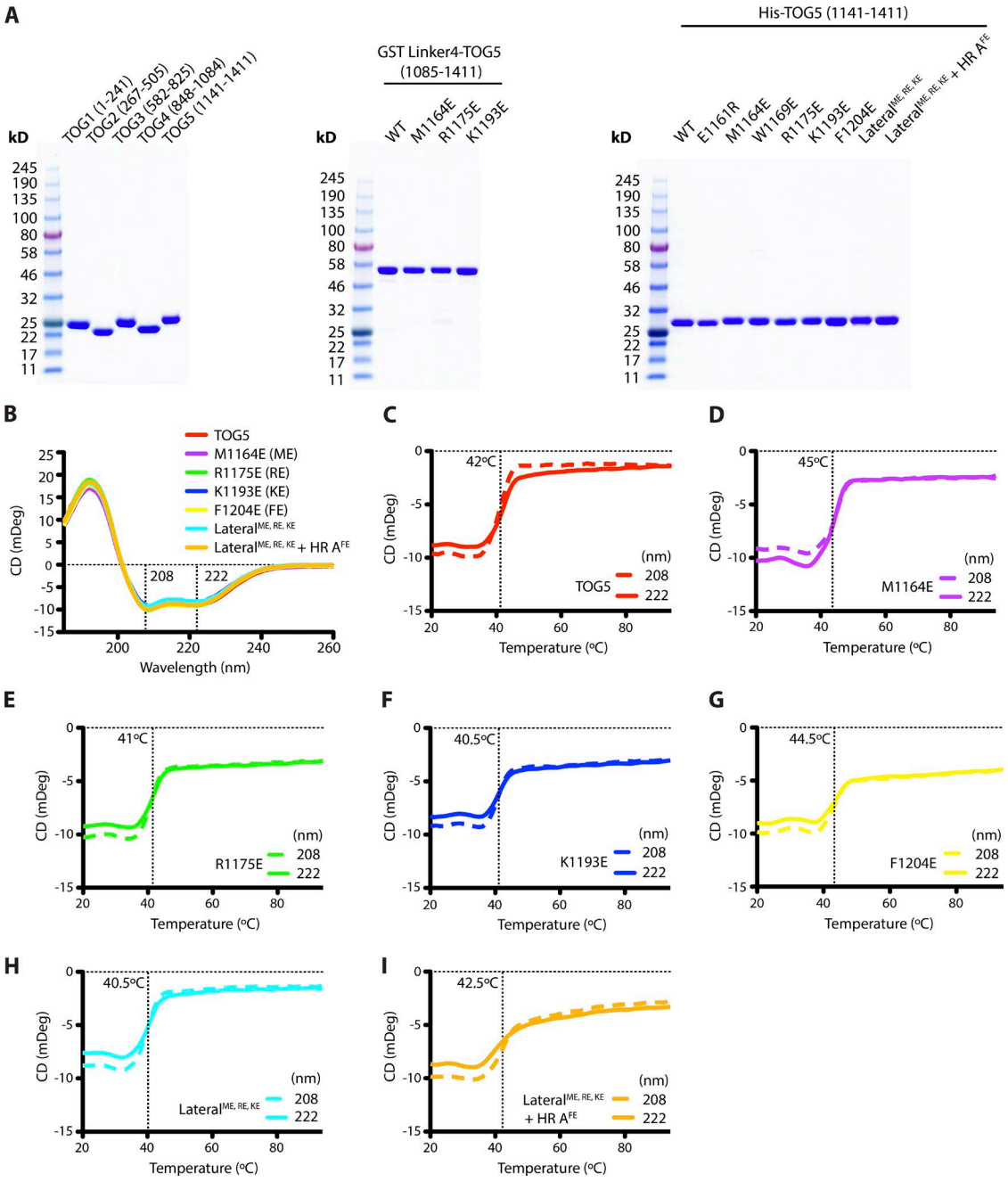

Figure S4. **Mutating TOG5–MT binding residues does not change domain secondary structure or stability.** (A) SDS gels of all purified TOG domain constructs used in this study. (B) CD spectra of native and mutant TOG5 constructs indicate α-helical secondary structure at 20°C, as shown by local minima at 208 and 222 nm. (C) The CD thermal melt of native TOG5 is cooperative and has an inflection point at 42°C. (D–I) Making single or multiple point mutations in TOG5 does not dramatically change TOG5's thermal melt profile. M1164E (D), R1175E (E), K1193E (F), and F1204E (G) single point mutation constructs have thermal melt profiles that show cooperative unfolding at 45°C, 41°C, 40.5°C, and 44.5°C, respectively. Multiple mutations in HR 0 (H) or HR 0 and HR A (I) do not change TOG5 stability.

Table S1. **Oligonucleotides**

Name	Sequence (5′ to 3′)
Msps 1141 NdeI F	GACTATCGTCATATGGATATCGACACATCGCCGCTACTGTGC
Msps 1411 XhoI R	GACTATCGTCTCGAGCTACTTAGTCTTTTTGGCTCGC
Msps 1085 BamHI F	GACTATCGTGGATCCGTAAAACCGCTGCCCAAAGGC
Msps 1411 NotI R	GACTATCGTGCGGCCGCTTACTTAGTCTTTTTGGCTCGC
GST GW F	CACCATGTCCCCTATACTAGGTTATTGG
Msps 1411 GW R	CTTAGTCTTTTTGGCTCGCTTGATGC
Msps R1157E F	GCCAACAGTGCTAAAAACCAGGAACTGCTAGACGAGCAAAAAATG
Msps R1157E R	CATTTTTTGCTCGTCTAGCAGTTCCTGGTTTTTAGCACTGTTGGC
Msps E1161R F	CCAGCGGCTGCTAGACCGCCAAAAAATGAAGGTAC
Msps E1161R R	GTACCTTCATTTTTTGGCGGTCTAGCAGCCGCTGG
Msps M1164E F	CTGCTAGACGAGCAAAAAGAGAAGGTACTAAAGTGGAC
Msps M1164E R	GTCCACTTTAGTACCTTCTCTTTTTGCTCGTCTAGCAG
Msps W1169E F	GAAGGTACTAAAGGAGACTTTTGTAACCC
Msps W1169E R	GGGTTACAAAAGTCTCCTTTAGTACCTTC
Msps R1175E F	GACTTTTGTAACCCCAGAAGAGGAATTCACCGAAC
Msps R1175E R	GTTCGGTGAATTCCTCTTCTGGGGTTACAAAAGTC
Msps K1193E F	GACCGCAAACGTAAATGAAGCACTGATAGCCAAC
Msps K1193E R	GTTGGCTATCAGTGCTTCATTTACGTTTGCGGTC
Msps 5UTR dsRNA F	GACTATCGTGTCGACTAATACGACTCACTATAGGTGTGAGTAGCGGTCACACTG
Msps 5UTR dsRNA R	GACTATCGTGGTACCTAATACGACTCACTATAGGCATCAGAATTGTGATCCAAGTACC
Msps 3UTR dsRNA F	GACTATCGTGTCGACTAATACGACTCACTATAGGACTGTGCGCTTCCCGTAGCTA
Msps 3UTR dsRNA R	GACTATCGTGGTACCTAATACGACTCACTATAGGCGCATATAGTTCATGAGGATG
SK dsRNA F	GACTATCGTGTCGACTAATACGACTCACTATAGGAAATTGTAAGCGTTAATATTTTG
SK dsRNA R	GACTATCGTGGTACCTAATACGACTCACTATAGGAACAGTTGCGCAGCCTGAATGG
Mad2 dsRNA F	GACTATCGTGTCGACTAATACGACTCACTATAGGAATGGCTCTCGAAGAACATGATC
Mad2 dsRNA R	GACTATCGTGGTACCTAATACGACTCACTATAGGTTAAGTGCTCATCTTGTAGTTGACC
Klp61F dsRNA F	GACTATCGTGTCGACTAATACGACTCACTATAGGGACTCTGACATTGGCATCATACC
Klp61F dsRNA R	GACTATCGTGGTACCTAATACGACTCACTATAGGTTCGGTGTATTCCTTGAGC
Msps Δ34 (551–1,102) F	ACAGGGGCACGTAAGGTCTTGAAAAAACTAAAAACAGTGCGCGGCGGTGGAG
Msps Δ34 (551–1,102) R	CTCCACCGCCGCGCACTGTTTTTAGTTTTTTCAAGACCTTACGTGCCCCTGT
Msps Δ34 (551–1,127) F	ACAGGGGCACGTAAGGTCTTGAAAAAAGGACAAGACAAGCAGGTACCAGCGC
Msps Δ34 (551–1,127) R	GCGCTGGTACCTGCTTGTCTTGTCCTTTTTTCAAGACCTTACGTGCCCCTGT
Msps Δ5 (1,141–1,411) F	CAGGTACCAGCGCGCAAAAAGGACGAAAAGCCCACGCCACCGCCATCTGTTGAT
Msps Δ5 (1,141–1,411) R	ATCAACAGATGGCGGTGGCGTGGGCTTTTCGTCCTTTTTGCGCGCTGGTACCTG
Msps Δ12345 (1–1,411) F	AAGCAGGCTCCGCGGCCGCCCCCTTCACCAAGCCCACGCCACCGCCATCTGTTGAT
Msps Δ12345 (1–1,411) R	ATCAACAGATGGCGGTGGCGTGGGCTTGGTGAAGGGGGCGGCCGCGGAGCCTGCTT
Msps Δ12 (1–505) F	AAGCAGGCTCCGCGGCCGCCCCCTTCACCCCAAAGAAGGAGACACGACCTGCATCTGC
Msps Δ12 (1–505) R	GCAGATGCAGGTCGTGTCTCCTTCTTTGGGGTGAAGGGGGCGGCCGCGGAGCCTGCTT
Msps Δ345 (582–1,411) F	CCCTAGCCACGGAACGCGAAATAACCAAGCCCACGCCACCGCCATCTGTTGATGTGC
Msps Δ345 (582–1,411) R	GCACATCAACAGATGGCGGTGGCGTGGGCTTGGTTATTTCGCGTTCCGTGGCTAGGG
Msps Δ45 (848–1,411) F	AGCCGGAGAAGAGGAGCCCATTAATAAGCCCACGCCACCGCCATCTGTTG
Msps Δ45 (848–1,411) R	CAACAGATGGCGGTGGCGTGGGCTTATTAATGGGCTCCTCTTCTCCGGCT
Msps 12341 Vector F	AAGCCCACGCCACCGCCATCTGTTGAT
Msps 12341 Vector R	TTCGTCCTTTTTGCGCGCTGGTACCTG
Msps 12341 TOG1 F	CAGGTACCAGCGCGCAAAAAGGACGAAGAGTACAAGAAGTTGCCGGTG
Msps 12341 TOG1 R	ATCAACAGATGGCGGTGGCGTGGGCTTGGACTTTAGATATCTGGAGGGTTC
Msps 52345 Vector F	CAGCAGGAAAAGCAAGCGAAGATCGCCGATGCTGC
Msps 52345 Vector R	TGTGTCCTCGGCCATGGTGAAGGGGGCGG
Msps 52345 TOG5 F	CCGCCCCCTTCACCATGGCCGAGGACACAGATATCGACACATCGCCGCTACTG
Msps 52345 TOG5 R	GCAGCATCGGCGATCTTCGCTTGCTTTTCCTGCTGCTTAGTCTTTTTGGCTCGCTTGATGC

F, forward; GW, gateway; R, reverse.

References

Ayaz, P., X. Ye, P. Huddleston, C.A. Brautigam, and L.M. Rice. 2012. A TOG:αβ-tubulin complex structure reveals conformation-based mechanisms for a microtubule polymerase. *Science.* 337:857–860. http://dx.doi.org/10.1126/science.1221698

Cao, L., W. Wang, Q. Jiang, C. Wang, M. Knossow, and B. Gigant. 2014. The structure of apo-kinesin bound to tubulin links the nucleotide cycle to movement. *Nat. Commun.* 5:5364. http://dx.doi.org/10.1038/ncomms6364

Fox, J.C., A.E. Howard, J.D. Currie, S.L. Rogers, and K.C. Slep. 2014. The XMAP215 family drives microtubule polymerization using a structurally diverse TOG array. *Mol. Biol. Cell.* 25:2375–2392. http://dx.doi.org/10.1091/mbc.E13-08-0501

Liu, J.S., C.R. Schubert, X. Fu, F.J. Fourniol, J.K. Jaiswal, A. Houdusse, C.M. Stultz, C.A. Moores, and C.A. Walsh. 2012. Molecular basis for specific regulation of neuronal kinesin-3 motors by doublecortin family proteins. *Mol. Cell.* 47:707–721. http://dx.doi.org/10.1016/j.molcel.2012.06.025

Maurer, S.P., F.J. Fourniol, G. Bohner, C.A. Moores, and T. Surrey. 2012. EBs recognize a nucleotide-dependent structural cap at growing microtubule ends. *Cell.* 149:371–382. http://dx.doi.org/10.1016/j.cell.2012.02.049

Nawrotek, A., M. Knossow, and B. Gigant. 2011. The determinants that govern microtubule assembly from the atomic structure of GTP-tubulin. *J. Mol. Biol.* 412:35–42. http://dx.doi.org/10.1016/j.jmb.2011.07.029

Redwine, W.B., R. Hernández-López, S. Zou, J. Huang, S.L. Reck-Peterson, and A.E. Leschziner. 2012. Structural basis for microtubule binding and release by dynein. *Science.* 337:1532–1536. http://dx.doi.org/10.1126/science.1224151